

Article

Performance of Reinforced Concrete Beams Strengthened by Bidirectional Carbon-Fiber-Reinforced Polymers Based on Numerical Models

Jae Sang Moon ¹ , Da Young Kim ², Myeong Seop Ko ² and Changhyuk Kim ^{2,*} ¹ Structural Department, Yooshin Engineering Corporation, Seoul 06252, Republic of Korea² Department of Architectural Engineering, Inha University, Incheon 22212, Republic of Korea

* Correspondence: changhyuk@inha.ac.kr; Tel.: +32-860-7565

Abstract: The use of carbon-fiber-reinforced polymers (CFRPs) for the repair and rehabilitation of reinforced concrete (RC) structures has been receiving a lot of attention. Specifically, the shear strengthening of RC members based on CFRP materials has been treated as an effective and efficient strengthening method. Previous research projects focused on the shear strengthening of RC members with unidirectional CFRP strips. Although the effectiveness of a bidirectional CFRP layout compared to a unidirectional CFRP layout was discussed in several studies, these studies only investigated the issue based on experiments. Moreover, the parameters of the bidirectional CFRP layout were not clearly defined. This study investigates the performance of RC beams strengthened by bidirectional CFRP based on numerical models. A numerical model based on finite element analysis is designed. Using the numerical model, the parameters of the horizontal CFRP strips, such as the layouts of horizontal CFRP strips and the number of horizontal CFRP strips, are studied. The results show that the effect of horizontal CFRP strips is maximized if the strips are distributed along the depth. In contrast, the number of horizontal CFRP strips does not significantly affect the shear strength of RC members.

Keywords: CFRP strengthening; bidirectional layout; finite element method; shear strength

Citation: Moon, J.S.; Kim, D.Y.; Ko, M.S.; Kim, C. Performance of Reinforced Concrete Beams Strengthened by Bidirectional Carbon-Fiber-Reinforced Polymers Based on Numerical Models. *Polymers* **2023**, *15*, 1012. <https://doi.org/10.3390/polym15041012>

Academic Editor: Wahid Ferdous

Received: 27 January 2023

Revised: 9 February 2023

Accepted: 14 February 2023

Published: 17 February 2023



Copyright: © 2023 by the authors. Licensee MDPI, Basel, Switzerland. This article is an open access article distributed under the terms and conditions of the Creative Commons Attribution (CC BY) license (<https://creativecommons.org/licenses/by/4.0/>).

1. Introduction

Although the reinforced concrete structure has been an effective structural system in civil and architectural engineering for a century, the effects of loading and extreme environmental conditions such as earthquakes, typhoons, and floods cause the strength deterioration of the structure. Furthermore, the increase in aged structures (more than 30 years old) has led to the increasing need for structural rehabilitation methods for the structures. To regain the structural performance of RC structures cost effectively, the retrofitting/strengthening of the aging reinforced concrete structures is a must. Various techniques, including section enlargement [1], external prestressing [2], steel plate bonding [3–5], and bonding of materials such as fiber-reinforced polymers [6,7], have been applied to improve the performance of aged RC structures. Recently, the use of carbon-fiber-reinforced polymer (CFRP) materials has been widely applied due to their high workability, low cost, and high strength-to-weight ratio. The high corrosion resistance and low thermal conductivity of the CFRP also help engineers to choose the material for the maintenance of RC structures.

Recent studies have focused on understanding the parameters and conditions relating to the use of CFRP in RC structures. Since CFRP-based strengthening is known as an efficient method of shear strengthening [8], many researchers have studied the shear performance of RC structures with CFRP. The contribution of the CFRP materials to the shear strength of RC beams with different sizes was investigated by Abbasi et al. [9], and Leung et al. [10], Kim et al. [11], and Dirar et al. [12] studied the effect of CFRP

reinforcements relating to the span-to-depth ratio of RC structures. In addition, the effect of steel stirrups on CFRP-reinforced RC structures was considered by Mofidi and Chaallal [13], Chen et al. [14], and de Freitas Arcine et al. [15]. Research on how mechanical parameters of the CFRP, such as fiber ratio, fiber materials, fiber layer numbers, and thickness, are related to the shear strengthening of RC structures was conducted by Jin et al. [16], Ebadi-Jamkhaneh [17], Bousselham and Chaallal [18], and Deniaud and Cheng [19]. The effects of pattern parameters, such as the space and width of CFRP strips, were studied numerically and experimentally by Tanarslan and Altin [20], Mofidi and Chaallal [21], and Khalifa and Nanni [22]. Additionally, the relationship between the angle of the CFRP strips and the behavior of the RC beams was experimentally investigated by Norris et al. [23], Chaallal et al. [24], and Monti and Liotta [25]. In addition, the effect of CFRP on the flexural strength of RC structures was studied by Vrettos et al. [26], Sun et al. [27], Smith et al. [28], and Li et al. [29]. Furthermore, research on the anchors of CFRP-strengthened structures was performed by Zhou et al. [30], Zhang and Smith [31], Sun et al. [32], Mostafa and Razaqpur [33], Pudleiner et al. [34], Li et al. [35], and Tatar et al. [36]. In addition, research on the CFRP debonding caused by various environmental conditions has recently been conducted by Zhang et al. [37], Al-lami et al. [38], and Yin et al. [39].

Most of the above studies evaluated the effect of unidirectional (vertical) CFRP strips. Compared to this, the studies on the use of bidirectional CFRP have been limited. Research papers have provided evidence of superior performances of bidirectional CFRP compared to those of unidirectional CFRP [4,40–49]. Kim et al. [40] experimentally compared the shear strengthening performance of unidirectional CFRP and bidirectional CFRP applied to I-girders. In this study, the increase in shear capacity achieved by bidirectional CFRP (up to 40%) is significantly higher than that achieved by unidirectional CFRP. A compression test of RC panels strengthened by bidirectional CFRP strips was also performed by Kim et al. [41,44] to investigate the bottle-shaped compression strut mechanism. The mechanism is easily seen in the web elements of deep RC beams. The test revealed that both the cracking loads and maximum loads of the panel were increased significantly with bidirectional CFRP. Later, Alotaibi [42] tested eight sets of RC T-beams strengthened with anchored bidirectional CFRP strips to examine the behavior. The research project presented the effectiveness of bidirectional CFRP strips related to the shear span–depth ratio of RC structures. These observations were the first attempts at investigating bidirectional CFRP. Furthermore, Haroon et al. [45] applied bidirectional CFRP strips to rectangular RC beams. The study experimentally investigated how the configuration of CFRP strips and stirrups affects the structural performance of RC beams. In addition, several studies investigated bidirectional CFRP strengthening. Rasheed et al. discussed the layout of bidirectional CFRP strips for T-beams [46]. Kalfat et al. studied the anchor system to prevent debonding [47]. Yilmaz et al. and Al-Atta et al. investigated bidirectional CFRP for slabs [48,49]. However, the studies on bidirectional CFRP strengthening are still relatively insufficient. Furthermore, they have studied the performance of bidirectional CFRP based on experiments. To define the mechanism that provides improved performance, the numerical study of bidirectional CFRP with proper mechanical models is required. Moreover, these studies have provided a few tests where the studied parameters of bidirectional CFRP strips are limited. Parameters such as the layout of horizontal CFRP and the thickness of the horizontal CFRP strips must be studied for the effective strengthening of RC structures.

The main objective of this study is to simulate the performance of RC beams strengthened by bidirectional CFRP based on numerical models. A set of RC beams with different patterns of CFRP is tested experimentally. The tested beams are numerically modeled based on finite element analysis. The numerical model is validated by comparing the result with the experiments. The numerical tests, based on the validated numerical model, are conducted to examine the parameters of the horizontal CFRP strips on RC beams. Parameters studied in this study include the layouts of horizontal CFRP strips and the number of horizontal CFRP strips.

2. Experimental Program

2.1. Code Provisions (ACI 318, 440.2R)

Since the number of experimental studies regarding bidirectional CFRP is limited, this study designed an experimental program to define the mechanism of bidirectional CFRP strips for RC beams and to verify the numerical model. To check the validity of the experiment, the design shear strengths of the test specimen were calculated and compared with the test results. In general, the shear strength of RC beams can be estimated using ACI 318-19 [50]. In general, the nominal shear strength of the RC beam, V_n , is the summation of shear strength provided by concrete (V_c) and shear reinforcement (V_s). In the code, the shear strength provided by concrete is calculated as follows:

$$V_c = \begin{cases} \text{Either of } \left\{ \begin{array}{l} \left[0.17\lambda\sqrt{f'_c} + \frac{N_u}{6A_g} \right] b_w d, \\ \left[0.66\lambda_s\lambda(\rho_w)^{1/3}\sqrt{f'_c} + \frac{N_u}{6A_g} \right] b_w d, \end{array} \right. & \text{for } A_v \geq A_{v,min} \\ \left[0.66\lambda_s\lambda(\rho_w)^{1/3}\sqrt{f'_c} + \frac{N_u}{6A_g} \right] b_w d, & \text{for } A_v < A_{v,min} \end{cases} \quad (1)$$

where b_w and d indicate the width and reinforcement depth of the rectangular section, respectively. f'_c is the compressive strength of the concrete. A_v is the area of shear reinforcement within spacing s in the RC beams. $A_{v,min}$ is the minimum area of shear reinforcement within spacing s for the design. ρ_w presents the ratio of A_s , the area of longitudinal section reinforcement, to the area of the section $b_w d$. A_g is the gross area of the concrete section, and N_u is the axial force which is normal to the cross-section, occurring simultaneously with shear force. N_u is positive for compression and negative for tension. λ and λ_s are the modification factors for the lightweight concrete and the size effect, respectively. Note that the maximum of both λ and λ_s is 1. Compared to the previous version of ACI 318 (ACI 318-14) [51], the equations of V_c have been simplified, since the previous code provided different equations depending on the axial loads.

The shear strength provided by shear reinforcement, which was not changed compared to the previous version, is defined in terms of A_v , f_{yt} , d , s , and α , the angle between stirrups and the longitudinal axis.

$$V_s = \frac{A_v f_{yt} (\sin \alpha + \cos \alpha) d}{s} \quad (2)$$

To estimate the shear strength of the RC beams strengthened by CFRP, not only V_c and V_s but also the shear strength provided by the CFRP must be defined. ACI 440.2R-17 [52] provides formulas to calculate the contribution of the CFRP in relation to the shear strength of the structure. When the RC structure is strengthened with CFRP, the nominal shear strength of the structure can be redefined as follows:

$$V_n = V_c + V_s + \psi_f V_f \quad (3)$$

V_f is the shear strength provided by the CFRP, and ψ_f is the reduction factor which is applied to the contribution of the CFRP system. A ψ_f of 0.85 is recommended for a three-sided U-wrap or two-opposite-sides strengthening schemes, while a ψ_f of 0.95 is recommended for completely wrapped members. The reduction factor for completely wrapped members is higher since the scheme is less bond dependent. Similar to V_s , V_f is defined as follows:

$$V_f = \frac{A_{fv} f_{fe} (\sin \alpha_f + \cos \alpha_f) d}{s_f} \quad (4)$$

where α_f is the angle between CFRP laminates and longitudinal direction. A_{fv} is the cross-sectional area of the CFRP laminates with spacing s_f . For the CFRP of rectangular sections, A_{fv} is the function of the width (w_f), thickness (t_f), and number (n_f) of the CFRP

laminates ($A_f = 2n_f t_f w_f$). f_{fe} is the effective stress in the CFRP at section failure. f_{fe} is directly proportional to the strain, which can be developed in the CFRP laminates at nominal strength.

$$f_{fe} = E_f \varepsilon_{fe} \quad (5)$$

where E_f is the tensile modulus of elasticity of CFRP, and ε_{fe} is the failure strain of the CFRP. For RC beams completely wrapped by CFRP, ε_{fe} is 0.004 and should be lower than 75% of the CFRP's rupture failure strain, $\varepsilon_{fu} (\leq 0.75\varepsilon_{fu})$. If CFRP systems do not wrap the entire section, ε_{fe} is defined using the bond reduction coefficient κ_v .

$$\varepsilon_{fu} = \kappa_v \varepsilon_{fu} \leq 0.004 \quad (6)$$

The bond reduction coefficient is defined in terms of the concrete strength, the wrapping scheme, and the stiffness of the laminate.

2.2. Specimen Detail

The study focused on numerical modeling which can describe the mechanism of bidirectional CFRP strips. The experiment tested the specimens with bidirectional CFRP layouts under different CFRP configurations. Additionally, the experiment included specimens with unidirectional CFRP strips under the same configurations. The specimens used in this study were the same as the test specimens used by Haroon et al. [39]. The main variables of this study included CFRP layouts, number of CFRP layers, and wrapping configurations of CFRP strips. Figure 1 describes the nomenclature of the specimen in the experiment program. The first character represents the layout of the CFRP strip. The second character indicates the number of CFRP layers used, which was either 1 or 2. The third character describes the wrapping configuration of the CFRP.

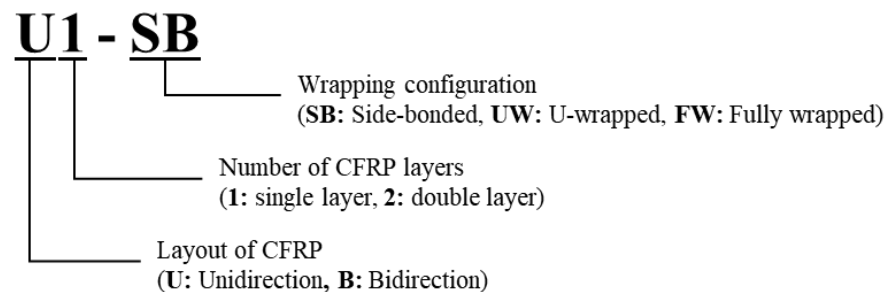


Figure 1. Nomenclature of test specimens.

Table 1 shows the details of the specimen. Tested RC beams had a cross-sectional dimension of 300×500 mm and a length of 2200 mm. The shear-span-to-depth ratio (a/d) of the specimen was 2.1. The compressive strength of the concrete (f'_c) measured from the cylindrical concrete specimen on the 28th day was 31.8 MPa. The elastic modulus of the concrete was 27,000 MPa. The width and spacing of the CFRP strips were 100 mm and 200 mm, respectively. The same width and spacing were applied to both vertical CFRP strips and horizontal CFRP strips. The mechanical properties of the CFRP strips were tested according to ASTM D 3039. The tensile strength and elastic modulus of CFRP strips from the test were 4600 MPa and 288,900 MPa, respectively.

Table 1. Experimental program specimen details.

Specimen	Concrete				CFRP Strip			
	b (mm)	h (mm)	f'_c (MPa)	$w_{f,v}$ (mm)	b (mm)	h (mm)	f'_c (MPa)	$w_{f,v}$ (mm)
U1-SB	300	500	31.8	100	200	N/A	N/A	4600
U1-UW	300	500	31.8	100	200	N/A	N/A	4600
U1-FW	300	500	31.8	100	200	N/A	N/A	4600
U2-FW	300	500	31.8	100	200	N/A	N/A	4600
B1-SB	300	500	31.8	100	200	100	200	4600
B1-UW	300	500	31.8	100	200	100	200	4600
B1-FW	300	500	31.8	100	200	100	200	4600
B1-FW(2)	300	500	31.8	100	200	100	200	4600

Note: b : width of RC beam, h : height of RC beam, $w_{f,v}$: vertical CFRP strip width, $s_{f,v}$: vertical CFRP strip spacing, $w_{f,h}$: horizontal CFRP strip width, $s_{f,h}$: horizontal CFRP strip spacing.

Figure 2 shows the specimen test region, CFRP layout, and experiment lab image. Since the test focused on shear failure, the flexural capacity of the beams was designed to be higher than the shear capacity of the beams by adding sufficient longitudinal reinforcement. D25 reinforcing bars with a yield strength of 400 MPa and an elastic modulus of 195,000 MPa were used for flexural reinforcement. The loading point was located 1020 mm from the left end of the beam, which was not symmetric. The left shear span, from the loading point to the left support, was designed to be the test region. The left span was designed to show shear failure prior to the right span. The shear reinforcement of the left span was designed using D6 rebars with 200 mm spacing, while the reinforcement of the right span was designed using D13 rebars with 100 mm spacing. B1-FW (2) had a bidirectional CFRP layout of three horizontal lines, while other bidirectional layouts had two horizontal lines of strips.

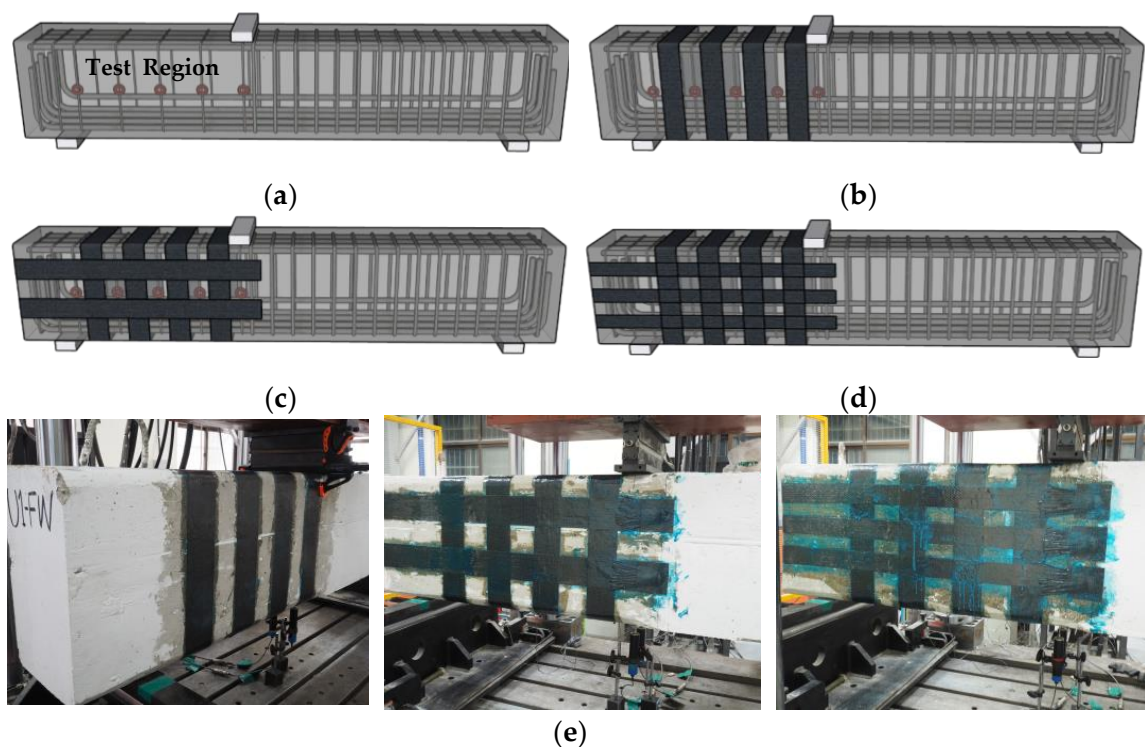


Figure 2. Test specimens and CFRP layout: (a) test region; (b) unidirectional CFRP layout; (c) bidirectional CFRP layout; (d) bidirectional CFRP layout (B1-FW(2)); (e) experiment specimens.

2.3. Test Equipment and Test Setup

The shear tests of specimens were conducted using a universal testing machine (UTM, AceoneTech, Incheon, Republic of Korea). The specimens were placed on two simple supports, and a steel plate was located on the loading point of the specimen described above. Figure 3 shows the location of the linear voltage displacement transducers (LVDTs) and strain gauge for the test. LVDTs were installed below the loading point to observe the deflection of the specimens. Five strain gauges were attached to the stirrups in the test region to measure the strain of transverse reinforcement. The strain gauges for CFRP strain measurement were attached in the same position as the strain gauge attached to the stirrups in the test region. Additionally, two strain gauges were attached to the longitudinal reinforcement at the loading point. The loading of the test specimens was achieved under a monotonic loading protocol. The specimens were unloaded when the beams reached 85% of the maximum load in the post-peak loading range. The loading was controlled to increase the deflection at a rate of 0.01 mm/sec.

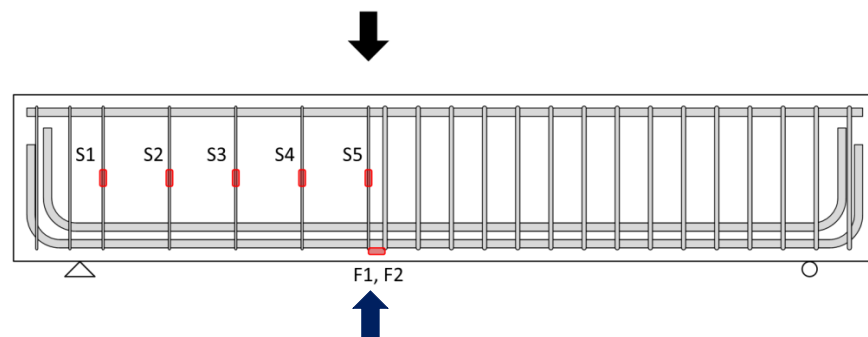


Figure 3. Test measurement (LVDTs and strain gauges).

2.4. Test Results

This section presents the test results of the CFRP-strengthened specimens. This study focused on the development of a numerical model which can describe the shear behavior of specimens. The results of the test were used for the validation of numerical models. This study summarizes the test results, and the details of the test results can be found in the previous study [45].

Table 2 shows the test results, including measured maximum strains of stirrups and strips and maximum loadings. Maximum loadings of the specimens were compared with the design capacity described in Section 2.1. The stirrups of all specimens reached the yield strain prior to the failure occurring. The test results showed higher shear capacity compared to the design shear capacity defined in ACI 318 codes. The shear ratios ($V_{\text{test}}/V_{\text{ACI}}$) were between 1.43 and 2.01. ACI 318-19 estimates the shear capacity of structures conservatively, which is reasonable.

Table 2. Test results.

	V_{ACI} (kN)	V_{test} (kN)	$V_{\text{test}}/V_{\text{ACI}}$	$\epsilon_{s,\text{max}}$	$\epsilon_{f,\text{max}}$
U1-SB	212	304	1.43	0.0046	0.0062
U1-UW	213	332	1.56	0.0033	0.0073
U1-FW	219	400	1.83	0.0040	0.0170
U2-FW	269	542	2.01	0.0031	0.0103
B1-SB	212	310	1.46	0.0075	0.0047
B1-UW	213	321	1.50	0.0094	0.0024
B1-FW	219	414	1.89	0.0142	0.0103
B1-FW(2)	219	429	1.96	0.0113	0.0095

Figure 4 presents the load deflection behavior of the specimens. For the figure, shear force (y-axis) was calculated from the applied point load. In the test, the maximum

shear forces of bidirectionally strengthened specimens did not show significant differences compared to those of unidirectionally strengthened specimens. However, the maximum deflections of bidirectionally strengthened specimens, with the maximum value on the x-axis, were larger than those of unidirectionally strengthened specimens. The maximum strains of the vertical CFRP strips shown in Table 2 were also higher when the bidirectional CFRP layout was applied. This reveals that the addition of horizontal CFRP strips can increase the ductility of a structure, which is preferable structural behavior.

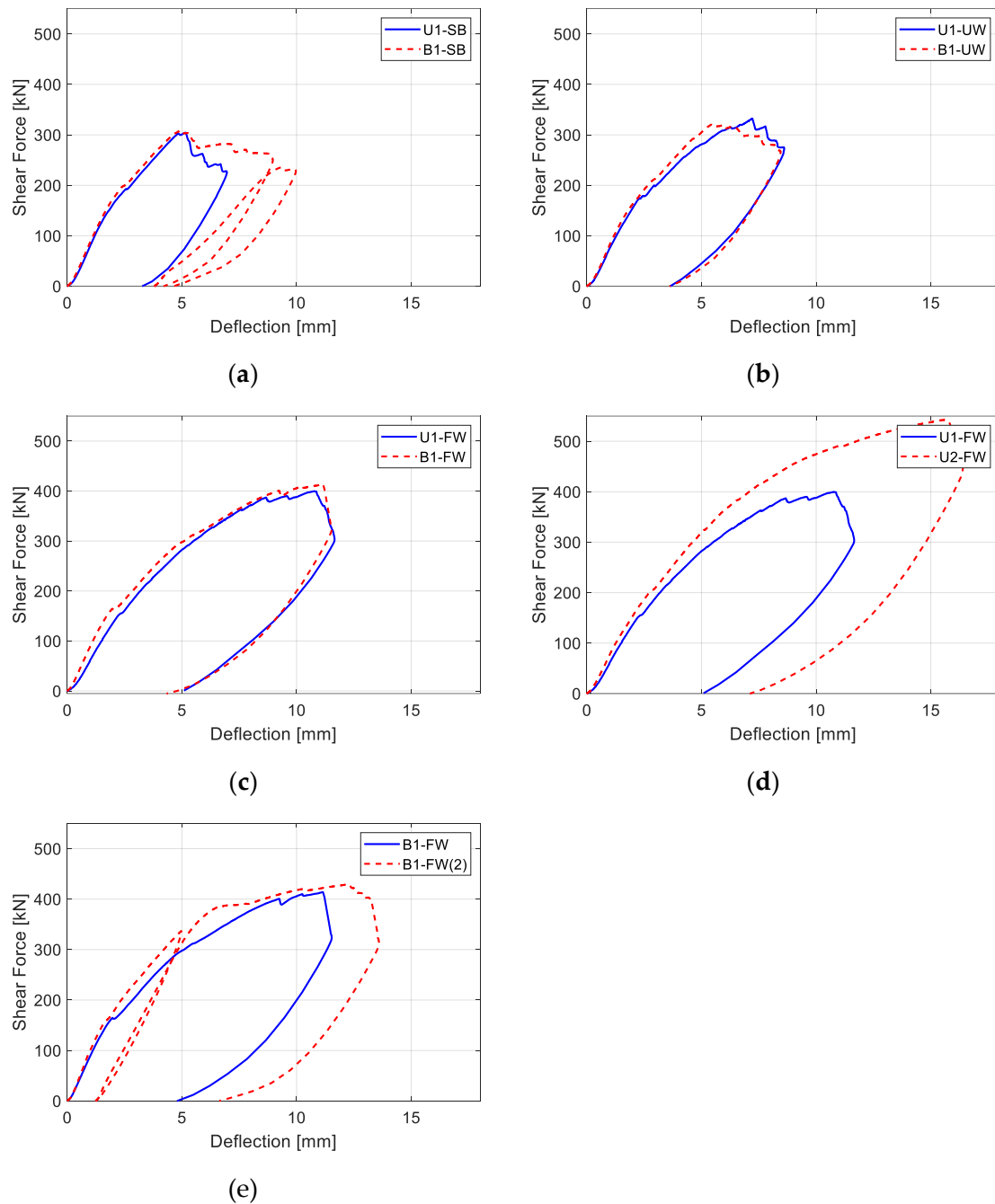


Figure 4. Load deflection behavior of specimens: (a) U1-SB vs. B1-SB; (b) U1-UW vs. B1-UW; (c) U1-FW vs. B1-FQ; (d) U1-FW vs. U2-FW; (e) B1-FW vs. B1-FW(2).

Figure 5 presents the measured CFRP strains of the test specimens according to the stirrup location. CFRP 1 is the strain of the CFRP located near the left reaction point of the specimen, while CFRP 4 is the strain of the CFRP located near the loading point of the

specimen. Lines with different colors represent the strains at different loading levels. At a loading level of 300 kN, the measured strain of all specimens, except U2-FW and B1-FW(2), reached the yield strain. The results indicate that the layout and configuration of CFRP strips affected the performance of the specimens. The maximum CFRP strains at a fixed load level were smaller in all specimens with bidirectional CFRP layouts than in specimens with unidirectional CFRP layouts. Additionally, side-bonded specimens showed lower maximum strains than fully wrapped and U-wrapped specimens. This is due to the failure modes of the specimens. The CFRP strips of the side-bonded specimens were delaminated before the CFRP strips reached maximum strain. For the complete analysis of the test, not only the CFRP strains but also the stirrup strains must be analyzed. The results and discussion regarding stirrup strains are provided by Haroon et al. [39].

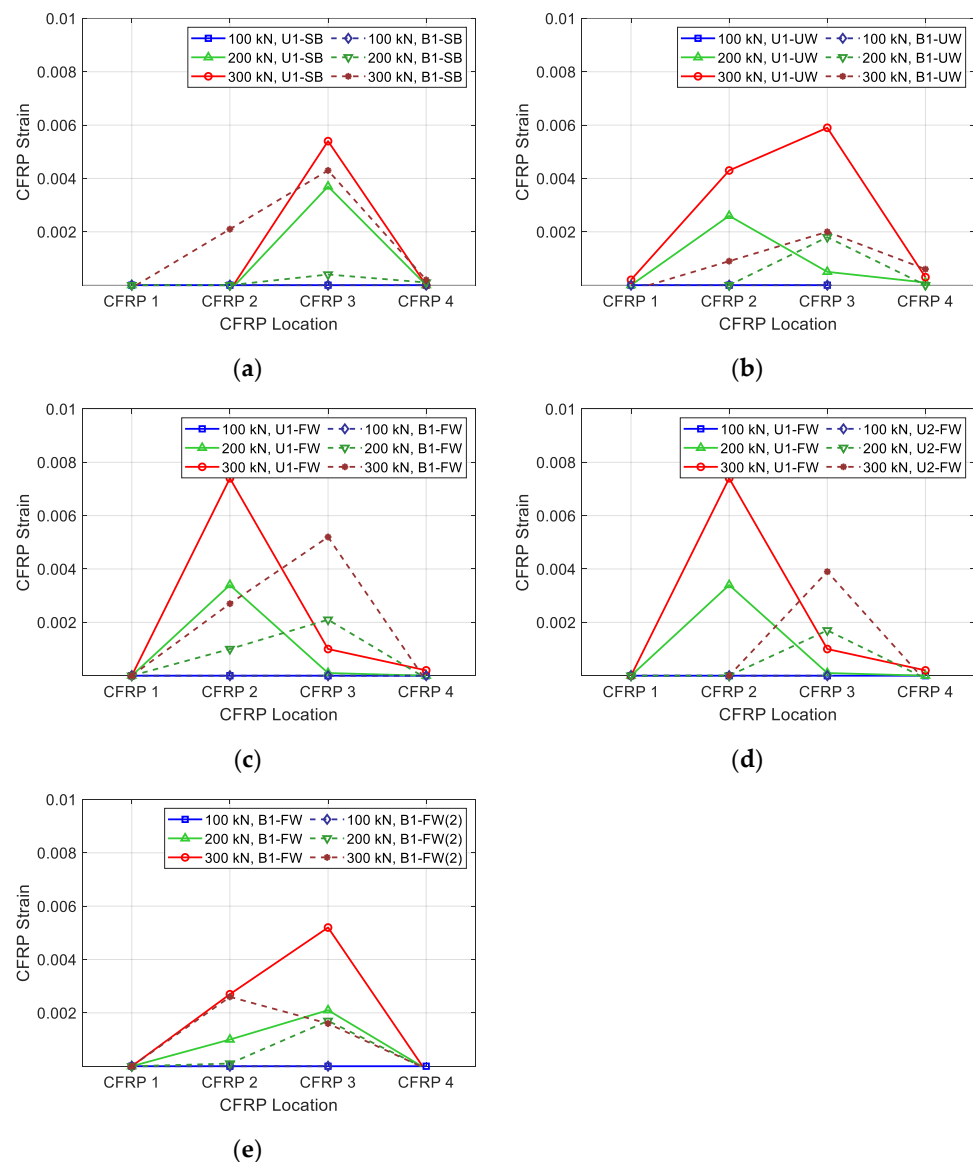


Figure 5. Measured CFRP strip strains of specimens: (a) U1-SB vs. B1-SB; (b) U1-UW vs. B1-UW; (c) U1-FW vs. B1-FQ; (d) U1-FW vs. U2-FW; (e) B1-FW vs. B1-FW(2).

3. Finite Element Analysis

The objective of this study was to numerically investigate the parameters of CFRP strengthening, which were not discussed in the previous study [45]. The numerical model for the CFRP-reinforced concrete beams was validated by comparing the model to the test

results of the previous study. To construct the numerical model for the CFRP-reinforced concrete beams, the program ATENA 3D (Cervenka, Praha, Czech Republic) [53] was utilized. ATENA 3D is nonlinear finite element analysis software that is widely used in the numerical study of concrete structures [54–58]. In this study, the CFRP-strengthened RC beams were modeled using the brick element (concrete) and shell element (CFRP strips). Figure 6 presents the modeling of the specimen. The gray element represents the concrete with reinforcements, and the orange element represents the CFRP strips.

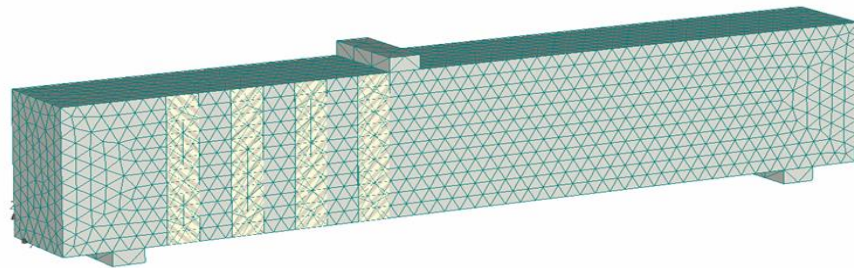


Figure 6. FEM modeling using ATENA 3D.

For the modeling of concrete, brick and tetra meshes with the size of 0.1 m were used. CFRP strips were modeled using brick and tetra meshes with a mesh size of 0.1 m. The isotropic linear elastic material model was applied to the CFRP modeling. Between the CFRP strips and the concrete, a 3D interface describing the properties of epoxy was modeled. The model was constructed based on the study of Kalfat and Al-Mahaidi [59].

3.1. Validation of the Analysis Model

To validate the analysis model, the results of material tests and specimens from the previous study [39] were compared with the FEM model. Figure 7 shows the CFRP material test results of the FEM. In the figure, it can be seen that the FEM model showed similar load displacement behavior to the test result. Compared to the test result, the displacement of the FEM model still increased, even with a loading smaller than the maximum loading. This was caused by the displacement control mode used in the FEM. The FEM model would have shown a similar result to the test if the analysis had been performed based on the load control.

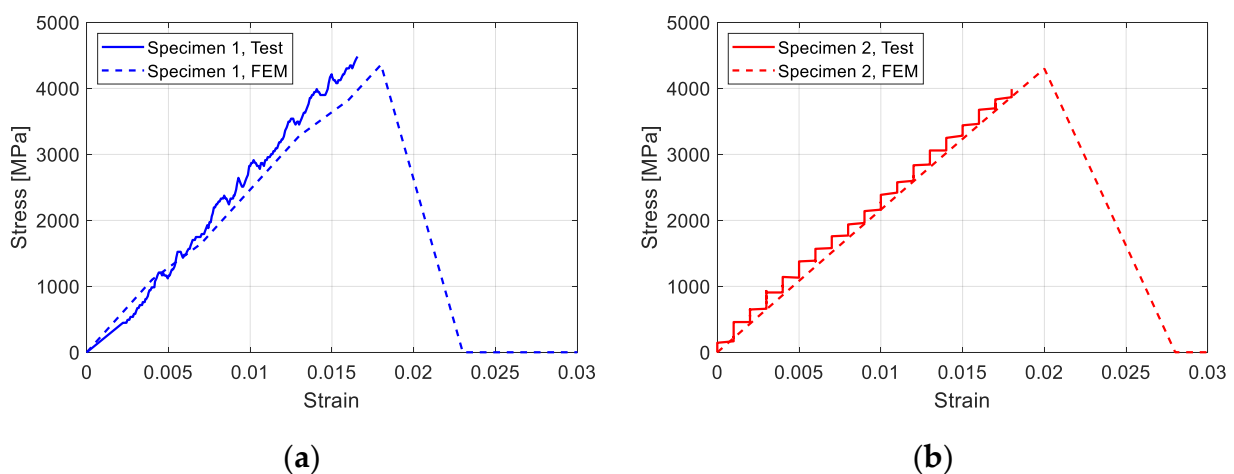


Figure 7. Test results of CFRP material: (a) CFRP specimen 1 (25 mm wide); (b) CFRP specimen 2 (50 mm wide).

Figures 8–11 present the strains of the stirrups and CFRP strips of the U1-SB, U1-FW, B1-SB, and B1-FW specimens at the different loading stages, respectively. The black,

horizontal dash line represents the yielding strain of the stirrups. In Figure 8, it can be seen that the distribution of strains at different specimen locations in the FEM model was different from that in the experiment. However, the maximum stirrup strains at each loading stage were similar for both the FEM model and the experiment (0.0027 vs. 0.0029 at 300 kN). In Figure 9, the distribution of both stirrups and CFRP strains at different specimen locations in the FEM model was similar to that in the experiment. The fully wrapped CFRP configuration provides a more stable performance than the side-bonded configuration because the configuration provides a larger area of contact between the CFRP and the concrete beam. Furthermore, the fully wrapped configuration provides higher CFRP strains due to the continuing effect provided by the CFRP strips. Figures 10 and 11, representing the results of the bidirectional CFRP layouts, show higher stirrup strains (0.0045 and 0.0039 at 300 kN) and lower CFRP strains (0.0043 and 0.0052 at 300 kN) compared to those in the unidirectional CFRP layouts. The overall results represent that the FEM model described the performance of the CFRP-strengthened beams well.

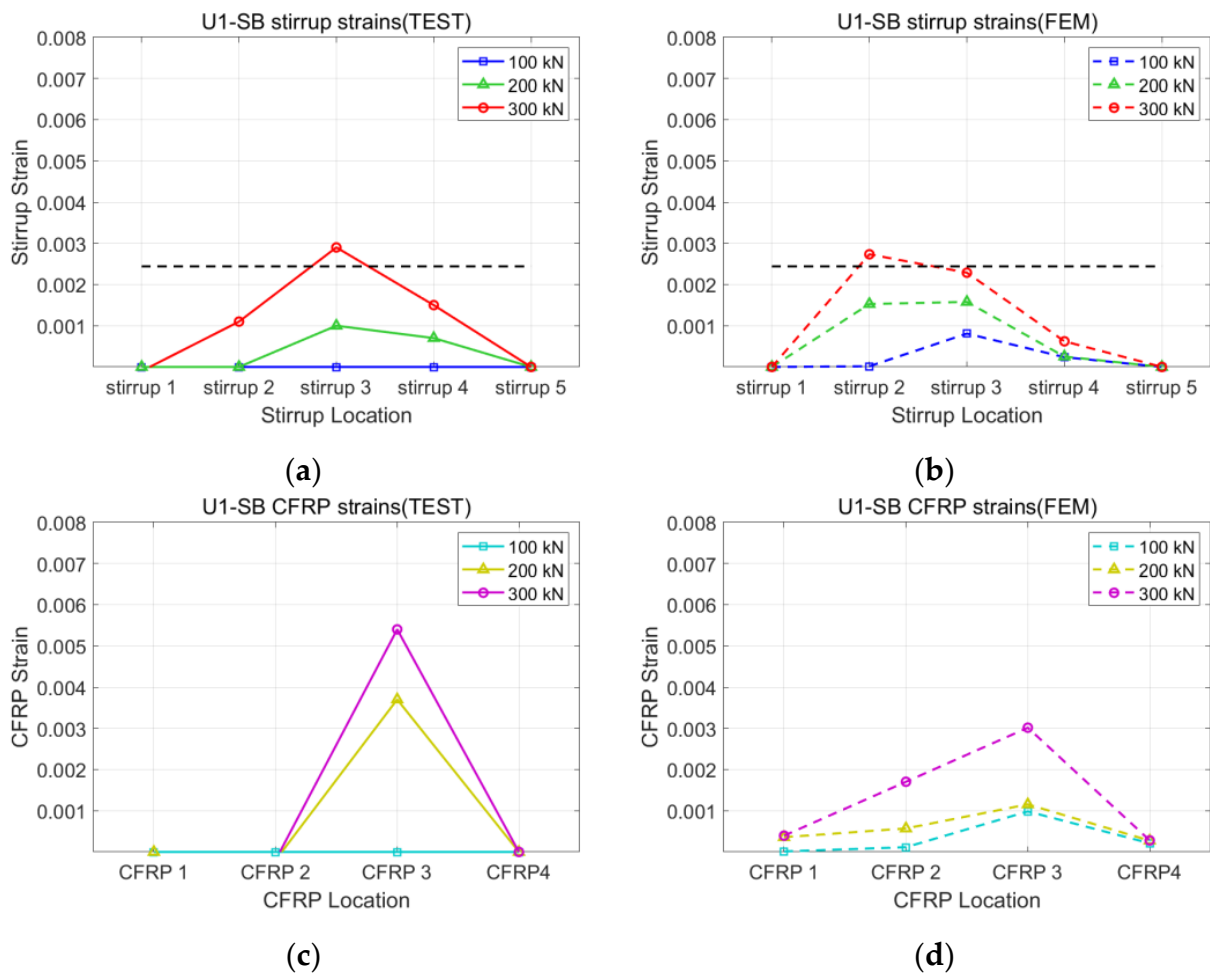


Figure 8. Strains of U1-SB specimen: (a) stirrup of test; (b) stirrup of FEM; (c) CFRP of test; (d) CFRP of FEM.

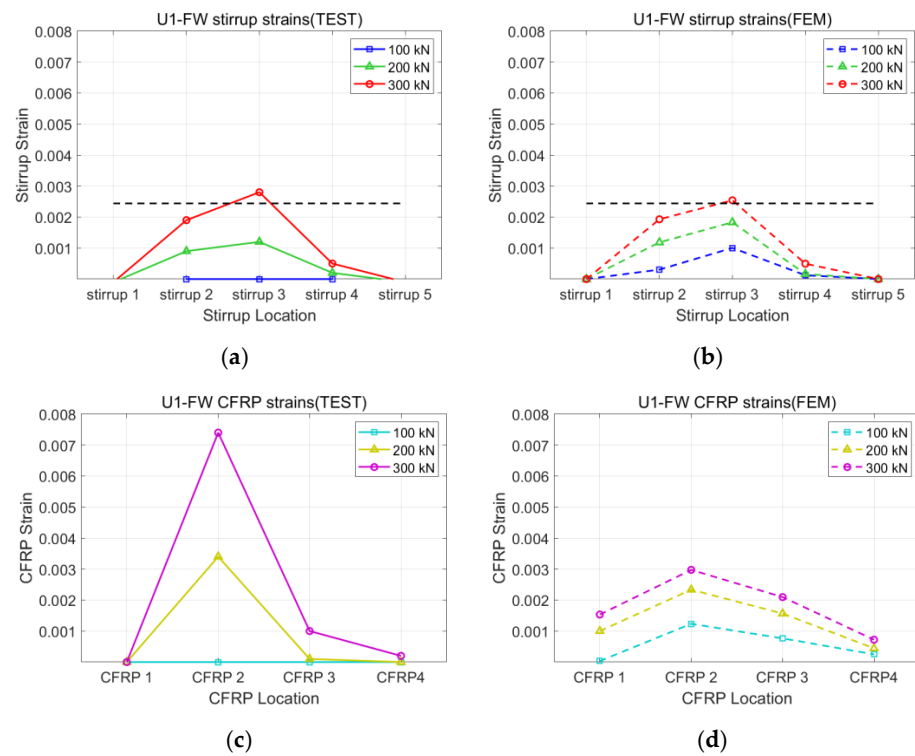


Figure 9. Strains of U1-FW specimen: (a) stirrup of test; (b) stirrup of FEM; (c) CFRP of test; (d) CFRP of FEM.

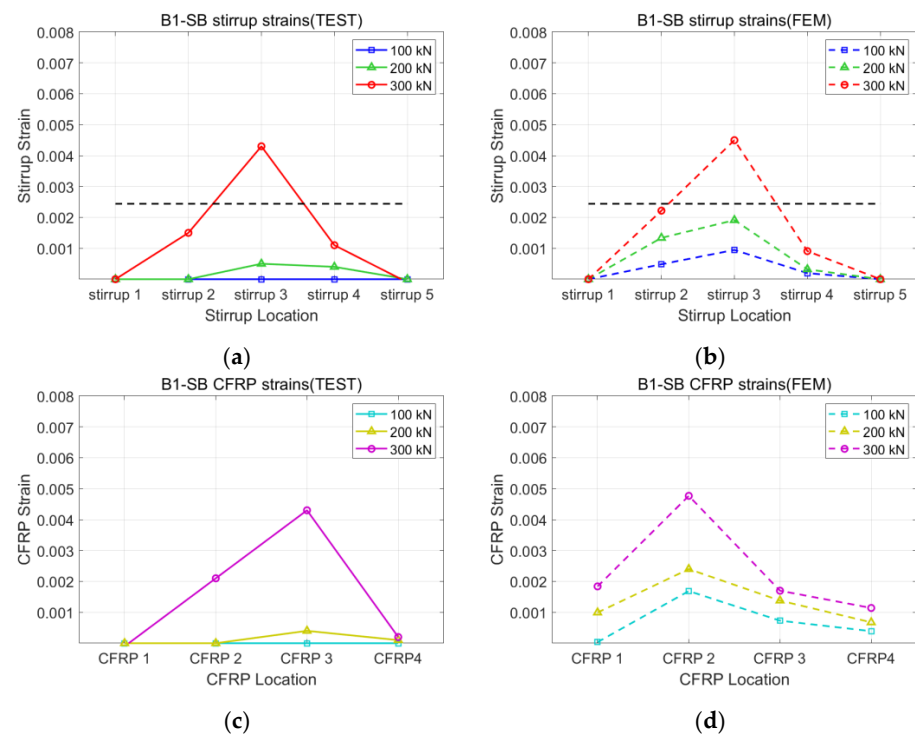


Figure 10. Strains of B1-SB specimen: (a) stirrup of test; (b) stirrup of FEM; (c) CFRP of test; (d) CFRP of FEM.

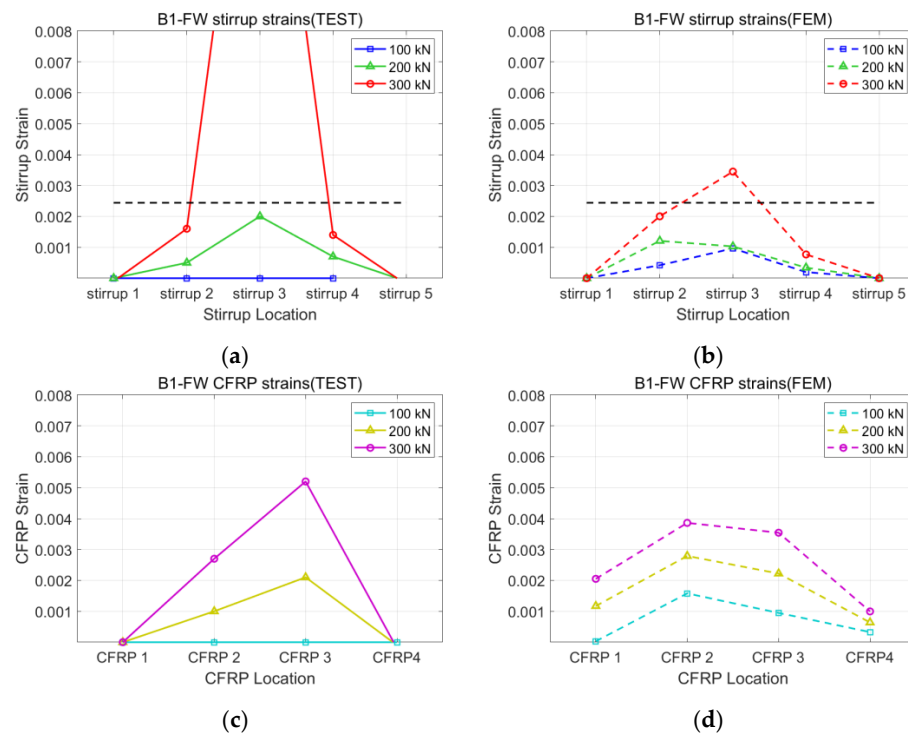


Figure 11. Strains of B1-FW specimen: (a) stirrup of test; (b) stirrup of FEM; (c) CFRP of test; (d) CFRP of FEM.

3.2. Parametric Study

As mentioned, the effect of CFRP layouts on RC beams could be simulated by utilizing the FEM software. Specifically, the effect of adding horizontal CFRP strips, which was not considered in the experimental study, was examined based on the numerical model. To evaluate the effect, parameters relating to the vertical CFRP strips, such as the number of layers and the wrapping configurations, were kept consistent. The parameters of the horizontal CFRP strips, such as layout and the amounts of materials, were numerically investigated in this study. Eight numerical models with different horizontal CFRP layouts and numbers of horizontal CFRP strips were constructed. All models used the same concrete beam used in the previous section. To clearly distinguish the effect of horizontal CFRP parameters, vertical CFRP strips with 70 mm width were fully wrapped to each RC beam model. All horizontal strips were modeled as fully bonded with both ends fixed to the RC beam. Figure 12 illustrates the horizontal CFRP layout patterns used in this study. For each model, the width of a single strip and the wrapping locations were modified, while the sums of the horizontal strip width for all models were the same. Figure 12a shows when two horizontal CFRP strips of 100 mm width were used. Figure 12b shows when three horizontal CFRP strips of 70 mm width were applied. Figure 12c,d show when a horizontal CFRP strip of 200 mm width was used. One strip was attached at the upper/bottom half of the RC beam. Single strip patterns were selected to investigate whether a wide single strip could strengthen the beam effectively. In practice, not all the beams could be reinforced, as shown in Figure 12a,b, due to site conditions. Therefore, Figure 12c,d represent the limited site conditions. If these patterns had shown the strengthening performance of the RC beam effectively, it would have been helpful for the site engineers. Figure 13 presents the nomenclature of the specimens in the parametric study, and Table 3 categorizes the details of the CFRP layout considered in this section. Strains of concrete and stirrups were compared to investigate the parameters of the horizontal CFRP strips.



Figure 12. Horizontal CFRP layout patterns: (a) distributed CFRP layout with two strips (100 mm); (b) distributed CFRP layout with three strips (70 mm); (c) on strip (200 mm) at bottom half; (d) one strip (200 mm) at the upper half.

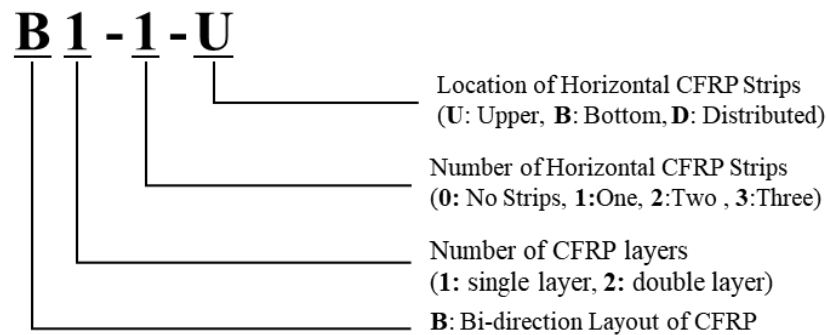


Figure 13. Nomenclature of test specimens for parametric study.

Table 3. CFRP strip parameters of numerical models.

Model		B1-2-D	B1-3-D	B1-1-B	B1-1-U	B2-2-D	B2-3-D	B2-1-B	B2-1-U
Horizontal CFRP	Total width (# × width) (mm)	200 (2 × 100)	210 (3 × 70)	200 (1 × 200)	200 (1 × 200)	200 (2 × 100)	210 (3 × 70)	200 (1 × 200)	200 (1 × 200)
	Thickness (mm)	0.3	0.3	0.3	0.3	0.6	0.6	0.6	0.6
Vertical CFRP	Total width (mm)	70, fully wrapped							
	Thickness (mm)	0.3							

Table 4 presents the results of the test, including maximum strains of stirrups and strips and maximum loadings. Similar to Table 2, the maximum loadings of the models were compared with the design capacity described in Section 2.1. The V_{test} of the control was measured from the experiment, while the other models were measured from the FEM. For $\epsilon_{f,max}$, the values in the bracket are the strain values for the horizontal CFRP strips. As seen in the table, the stirrup strains of all models were larger than the yield strain when the failure occurred. All the test results showed a higher shear capacity compared to the designed shear capacity defined. In terms of the shear ratios (V_{test}/V_{ACI}), all models with bidirectional CFRP strips showed higher values than the values of the control. The shear ratios of the models were between 1.70 to 1.85. In Sections 3.2.1 and 3.2.2, the results of the test are further discussed.

Table 4. Test results for parametric study.

Model	V_{ACI} (kN)	V_{test} (kN)	V_{test}/V_{ACI}	$\varepsilon_{s,max}$	$\varepsilon_{f,max}$
Control	219	307	1.40	0.0166	
B1-2-D	219	406	1.85	0.0093	0.0136(0.0124)
B1-3-D	219	398	1.82	0.0078	0.0110(0.0098)
B1-1-B	219	376	1.72	0.0150	0.0149(0.0121)
B1-1-U	219	397	1.81	0.0190	0.0160(0.0100)
B2-2-D	219	406	1.85	0.0089	0.0130(0.0129)
B2-3-D	219	405	1.85	0.0101	0.0130(0.0117)
B2-1-B	219	372	1.70	0.0129	0.0136(0.0133)
B2-1-U	219	399	1.82	0.0185	0.0157(0.0101)

(V_{test} for control is from the experimental study, while V_{test} for the other models is from the FEM).

3.2.1. Horizontal CFRP Layout

Figure 14 presents the distribution of concrete strains for the test specimens of different layouts. Control in the figure indicates the numerical model of the concrete beam strengthened with only vertical CFRP strips (no horizontal CFRP). In the figure, the high strain values of all specimens are concentrated around the diagonal crack between the left support and the left loading point. As expected, the control showed the highest strain values (0.0173) compared to the other cases. For B1-1-B and B1-1-U, the highest strains, of 0.009, were found at the upper half and the lower half of the beams, respectively. These were where the horizontal strips were not placed. Among the models with distributed horizontal CFRP strips, B1-3-D showed the lowest strain, 0.006, and the most evenly distributed results. The next lowest strain value was seen in B1-2-D (0.007). In the model, high strains were found between horizontal strips. These results indicate that the continuing effect of horizontal CFRP strips can be maximized when the strips are divided and placed widely along the depth of the concrete beam. If a wide strip is horizontally bonded aside due to the site condition, the other part without the horizontal strip is the weak point. For the effective strengthening of RC beams, horizontal strips must be bonded uniformly along the depth of the beam.

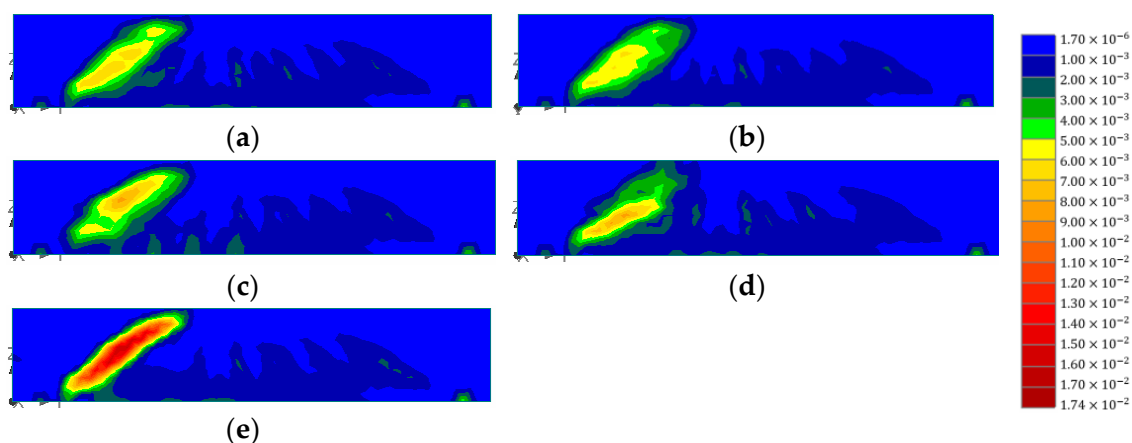


Figure 14. Comparison of concrete strains for different horizontal CFRP layouts: (a) B1-2-D; (b) B1-3-D; (c) B1-1-B; (d) B1-1-U; (e) control.

Figure 15 presents the stirrup strains for different CFRP layouts. The distribution of stirrup strains was examined to verify the continuing effect caused by the horizontal CFRP strengthening. The maximum strain value for the B1-2-D, B1-3D, B1-1-B, B1-1-U, and control models were 0.00219, 0.00207, 0.00201, 0.00223, and 0.00345, respectively. From the figure, it can be seen that models with horizontal CFRP presented similar stirrup strain distributions regardless of layout (highest strain at the top and higher stirrup 2 strain than

stirrup 4 strain at 300 kN). Stirrup strains of all models with horizontal CFRP showed lower strain values than those of the control at all loads. Furthermore, the stirrups of models with horizontal CFRP did not yield when the loading reached 300 kN, while the stirrup of the control showed a strain value higher than the yielding strain (0.00244).

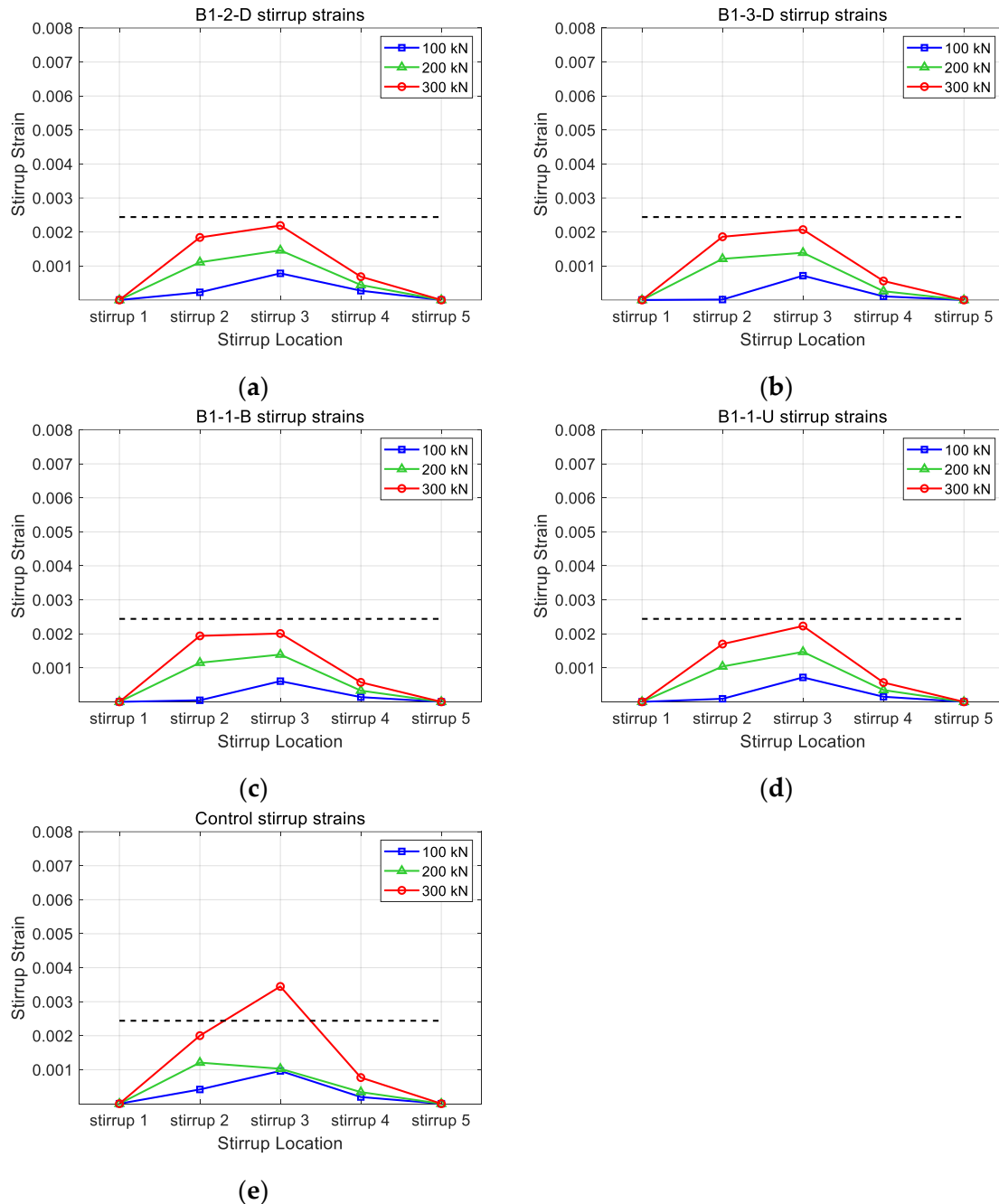


Figure 15. Comparison of stirrup strains for different horizontal CFRP layouts: (a) B1-2-D; (b) B1-3-D; (c) B1-1-B; (d) B1-1-U; (e) control.

3.2.2. Amount of Horizontal CFRP Layout

Figures 16 and 17 illustrate the concrete strain and stirrup strains with horizontal CFRP strips of 0.6 mm. As mentioned above, the vertical CFRP strips were fixed at 0.3 mm, and each thickness of the horizontal strips was set as 0.3 mm and 0.6 mm. In Figure 16, it can be seen that the patterns of concrete strains with different CFRP layouts showed similar patterns to those illustrated in Figure 14. The concentration of strains decreased

as the CFRP strips were added to the concrete. Not only the strain concentration patterns but also the maximum strain values were similar for horizontal CFRP layouts. Among the models with horizontal strips, the B2-3-D model showed the lowest strain value. The maximum strain values of the B2-3-D model were similar to those of the B1-3-D model. This indicates that the increase in thickness in horizontal CFRP strips did not improve the shear performance of specimens. Although the number of horizontal strips increased, the failure came from either the delamination of the vertical CFRP or the concrete. The increase in thickness of the horizontal CFRP strips could not delay the delamination of CFRP strips. In Figure 17, it can be seen that the maximum strain value for B2-2-D, B2-3-D, B2-1-B, and B2-1-U was 0.00218, 0.00214, 0.00212, and 0.00224, respectively. Figure 17 shows similar behavior. Except for the control model, stirrups did not reach the yield stress. The distribution patterns of stirrup strains were similar to those in Figure 15. Since the failure of the model came from the delamination, these are acceptable results.

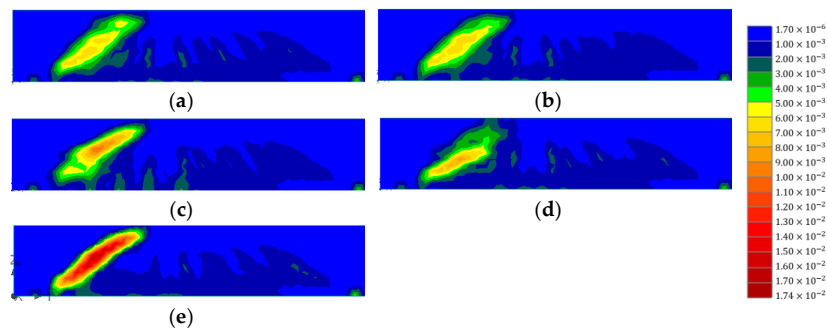


Figure 16. Comparison of concrete strains for different horizontal CFRP layouts: (a) B2-2-D; (b) B2-3-D; (c) B2-1-B; (d) B2-1-U; (e) control.

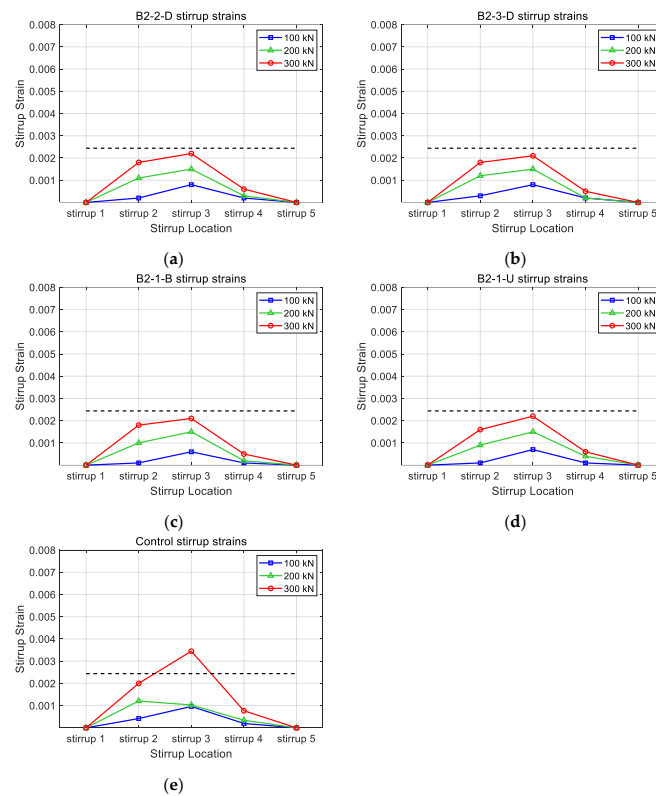


Figure 17. Comparison of stirrup strains for different horizontal CFRP layouts: (a) B2-2-D; (b) B2-3-D; (c) B2-1-B; (d) B2-1-U; (e) control.

4. Discussion

The results indicate that the layout of the horizontal CFRP affects the structural performance of RC beams significantly, while the number of horizontal CFRP strips does not significantly affect the structural performance. When a horizontal strip is located either at the bottom/upper half of the RC beam, the strips only confine the concrete and vertical strips in the located half. The horizontal strips cannot confine the other half where the high concrete strains are found. When the horizontal strip is divided into multiple strips and bonded uniformly along the depth, the effect of adding horizontal CFRP strips increases. Among the investigated models, the layout pattern with three strips provided the best performance. The pattern with three strips kept the vertical CFRP strips from debonding well compared to the others. Furthermore, the widely distributed horizontal CFRP strips confined the concrete beam and prevented the failure of the beam effectively.

Compared to the layout pattern, the number of horizontal CFRP strips cannot change the effect of horizontal CFRP strengthening. Even if the number of horizontal CFRP strip layers is doubled, the concrete strains and stirrup strains of the concrete do not decrease dramatically. The increased horizontal CFRP strip layers cannot delay the delamination of vertical CFRP strips. Although the increased horizontal strip amounts can confine the concrete for horizontal expansion, the conditions for vertical strip delamination are the same. The horizontal CFRP layout pattern becomes a more important parameter than the number of horizontal CFRP strips for the efficient strengthening of the RC beam. For the site project, the use of horizontal strips of a single layer around the depth of the beam instead of using a multiple-layered strip to a narrow location of the depth is recommended.

5. Conclusions

In this study, the effectiveness of bidirectional CFRP strengthening of rectangular RC beams was numerically investigated. The RC beams with CFRP strengthening were numerically modeled based on FEM. The constructed numerical models were validated by comparing them to the experiments. RC beams with unidirectional/bidirectional CFRP layout and side-bonded/fully wrapped vertical CFRP strips were used for the validation. Both the experiment and numerical model revealed that bidirectional CFRP provides improved performance compared to unidirectional CFRP. Based on the numerical model, the parameters such as the layout and amount of horizontal CFRP were studied. The layout of the horizontal CFRP is a more significant parameter than the amount of horizontal CFRP. From this study, the numerical model, which provided the performance of RC beams with bidirectional CFRP, was developed. The model can be used not only for parametric studies but also for the simulation of projects regarding CFRP strengthening of RC beams.

The following items are planned for future study. First, further study on the parameters relating to horizontal CFRP strips will be performed. Since the number of horizontal CFRP strips in this study did not show different performance, items such as the minimum number of horizontal CFRP strips for various RC beams will be studied. Next, a refinement of the numerical model will be developed. The development of a numerical model describing the behavior of CFRP-strengthened RC beams more accurately will be performed. Finally, the effect of bidirectional CFRP strengthening relating to dynamic loads will be investigated. The performance of CFRP-strengthened structures not only in relation to static loads but also to dynamic loads must be studied.

Author Contributions: Conceptualization, C.K.; methodology, C.K.; formal analysis, C.K.; investigation, J.S.M.; resources, C.K.; data curation, C.K., D.Y.K. and M.S.K.; writing—original draft preparation, J.S.M.; writing—review and editing, J.S.M.; visualization, D.Y.K. and M.S.K.; supervision, C.K.; project administration, C.K. All authors have read and agreed to the published version of the manuscript.

Funding: This work was supported by a National Research Foundation of Korea (NRF) grant funded by the Korea government (MSIT) (no. 2022R1C1C1009269).

Institutional Review Board Statement: Not applicable.

Data Availability Statement: All the research data used in this manuscript will be available whenever requested.

Conflicts of Interest: The authors declare no conflict of interest.

References

1. Yang, K.-H. Axial Behavior of Reinforced Concrete Columns Strengthened with New Section Enlargement Approaches. *ACI Struct. J.* **2019**, *116*, 87–96. [\[CrossRef\]](#)
2. Kaur, H.; Singh, J. A Review on External Prestressing in Concrete. *Int. Res. J. Eng. Technol.* **2017**, *4*, 1801–1805.
3. Vilnay, O. The Analysis of Reinforced Concrete Beams Strengthened by Epoxy Bonded Steel Plates. *Int. J. Cem. Compos. Lightweight Concr.* **1988**, *10*, 73–78. [\[CrossRef\]](#)
4. Adhikary, B.B.; Mutsuyoshi, H.; Sano, M. Shear Strengthening of Reinforced Concrete Beams Using Steel Plates Bonded on Beam Web: Experiments and Analysis. *Constr. Build. Mater.* **2000**, *14*, 237–244. [\[CrossRef\]](#)
5. Zhang, S.; Raoof, M.; Wood, L.A. Prediction of Peeling Failure of Reinforced Concrete Beams with Externally Bonded Steel Plates. *Proc. Inst. Civ. Eng.-Struct. Build.* **1995**, *110*, 257–268. [\[CrossRef\]](#)
6. Spoelstra, M.R.; Monti, G. FRP-Confined Concrete Model. *J. Compos. Constr.* **1999**, *3*, 143–150. [\[CrossRef\]](#)
7. Rizkalla, S.; Hassan, T.; Hassan, N. Design Recommendations for the Use of FRP for Reinforcement and Strengthening of Concrete Structures. *Prog. Struct. Eng. Mater.* **2003**, *5*, 16–28.
8. Bourget, S.; El-Saikaly, G.; Chaallal, O. Behavior of Reinforced Concrete T-Beams Strengthened in Shear Using Closed Carbon Fiber-Reinforced Polymer Stirrups Made of Laminates and Ropes. *ACI Struct. J.* **2017**, *114*, 1087. [\[CrossRef\]](#)
9. Abbasi, A.; Benzeguir, Z.E.A.; Chaallal, O.; El-Saikaly, G. FE Modelling and Simulation of the Size Effect of RC T-Beams Strengthened in Shear with Externally Bonded FRP Fabrics. *J. Compos. Sci.* **2022**, *6*, 116. [\[CrossRef\]](#)
10. Leung, C.K.Y.; Chen, Z.; Lee, S.; Ng, M.; Xu, M.; Tang, J. Effect of Size on the Failure of Geometrically Similar Concrete Beams Strengthened in Shear with FRP Strips. *J. Compos. Constr.* **2007**, *11*, 487–496. [\[CrossRef\]](#)
11. Kim, Y.; Quinn, K.; Ghannoum, W.M.; Jirsa, J.O. Strengthening of Reinforced Concrete T-Beams Using Anchored CFRP Materials. *ACI Struct. J.* **2014**, *111*, 1027. [\[CrossRef\]](#)
12. Dirar, S.; Lees Janet, M.; Morley, C. Phased Nonlinear Finite-Element Analysis of Precracked RC T-Beams Repaired in Shear with CFRP Sheets. *J. Compos. Constr.* **2013**, *17*, 476–487. [\[CrossRef\]](#)
13. Mofidi, A.; Chaallal, O. Effect of Steel Stirrups on Shear Resistance Gain Due to Externally Bonded Fiber-Reinforced Polymer Strips and Sheets. *Am. Concr. Inst. Struct. J.* **2014**, *111*, 353–361.
14. Chen, G.M.; Teng, J.G.; Chen, J.F.; Rosenboom, O.A. Interaction between Steel Stirrups and Shear-Strengthening FRP Strips in RC Beams. *J. Compos. Constr.* **2010**, *14*, 498–509. [\[CrossRef\]](#)
15. de Freitas Arcine, M.; Villanova Menon, N.; Augusto Krahl, P. Numerical and Experimental Study of the Interaction between Stirrups and Shear Strengthening with CFRP in RC Beams. *Eng. Struct.* **2023**, *278*, 115514. [\[CrossRef\]](#)
16. Jin, L.; Xia, H.; Jiang, X.; Du, X. Size Effect on Shear Failure of CFRP-Strengthened Concrete Beams without Web Reinforcement: Meso-Scale Simulation and Formulation. *Compos. Struct.* **2020**, *236*, 111895. [\[CrossRef\]](#)
17. Ebadi-Jamkhaneh, M.; Homaioon-Ebrahimi, A.; Kontoni, D.-P.N. Numerical Finite Element Study of Strengthening of Damaged Reinforced Concrete Members with Carbon and Glass FRP Wraps. *Comput. Concr.* **2021**, *28*, 137–147.
18. Bousselham, A.; Chaallal, O. Mechanisms of Shear Resistance of Concrete Beams Strengthened in Shear with Externally Bonded FRP. *J. Compos. Constr.* **2008**, *12*, 499–512. [\[CrossRef\]](#)
19. Deniaud, C.; Roger Cheng, J.J. Reinforced Concrete T-Beams Strengthened in Shear with Fiber Reinforced Polymer Sheets. *J. Compos. Constr.* **2003**, *7*, 302–310. [\[CrossRef\]](#)
20. Tanarlan, H.M.; Altin, S. Behavior of RC T-Section Beams Strengthened with CFRP Strips, Subjected to Cyclic Load. *Mater. Struct.* **2010**, *43*, 529–542. [\[CrossRef\]](#)
21. Mofidi, A.; Chaallal, O. Shear Strengthening of RC Beams with Externally Bonded FRP Composites: Effect of Strip-Width-to-Strip-Spacing Ratio. *J. Compos. Constr.* **2011**, *15*, 732. [\[CrossRef\]](#)
22. Khalifa, A.; Nanni, A. Improving Shear Capacity of Existing RC T-Section Beams Using CFRP Composites. *Cem. Concr. Compos.* **2000**, *22*, 165–174. [\[CrossRef\]](#)
23. Norris, T.; Saadatmanesh, H.; Ehsani, M.R. Shear and Flexural Strengthening of R/C Beams with Carbon Fiber Sheets. *J. Struct. Eng.* **1997**, *123*, 903–911. [\[CrossRef\]](#)
24. Chaallal, O.; Nollet, M.J.; Perraton, D. Shear Strengthening of RC Beams by Externally Bonded Side CFRP Strips. *J. Compos. Constr.* **1998**, *2*, 111–113. [\[CrossRef\]](#)
25. Monti, G.; Liotta, M. Tests and Design Equations for FRP-Strengthening in Shear. *Constr. Build. Mater.* **2007**, *21*, 799–809. [\[CrossRef\]](#)
26. Vrettos, I.; Kefala, E.; Triantailou, T.C. Innovative Flexural Strengthening of Reinforced Concrete Columns Using Carbon-Fiber Anchors. *ACI Struct. J.* **2013**, *110*, 63–70.
27. Sun, W.; Liu, S.; Zhang, C. An Effective Improvement for Enhancing the Strength and Feasibility of FRP Spike Anchors. *Compos. Struct.* **2020**, *247*, 112449. [\[CrossRef\]](#)

28. Smith, S.T.; Hu, S.; Kim, S.J.; Seracino, R. FRP-Strengthened RC Slabs Anchored with FRP Anchors. *Eng. Struct.* **2011**, *33*, 1075–1087. [[CrossRef](#)]
29. Li, G.; Zhang, A.; Jin, W.; Xiao, Y.; Li, H. A New Flexural Strength Model of CFRP-Strengthened RC Beams with Intermediate Crack Induced Debonding Failure. *Compos. Struct.* **2023**, *308*, 116681. [[CrossRef](#)]
30. Zhou, C.; Liu, J.; Yu, Y. Experiment and Modeling of RC Beams Shear-Strengthened with Hybrid-Anchored CFRP U-Straps. *Strain* **2017**, *1*, S3.
31. Zhang, H.W.; Smith, S.T. FRP-to-Concrete Joint Assemblages Anchored with Multiple FRP Anchors. *Compos. Struct.* **2012**, *94*, 403–414. [[CrossRef](#)]
32. Sun, W.; Jirsa, J.O.; Ghannoum, W.M. Behavior of Anchored Carbon Fiber-Reinforced Polymer Strips Used for Strengthening Concrete Structures. *ACI Mater. J.* **2016**, *113*, 163–172. [[CrossRef](#)]
33. Mostafa, A.; Razaqpur, A.G. CFRP Anchor for Preventing Premature Debonding of Externally Bonded FRP Laminates from Concrete. *J. Compos. Constr.* **2013**, *17*, 641–650. [[CrossRef](#)]
34. Pudleiner, D.; Ghannoum, W.M.; Jirsa, J.O. Influence of Anchor Size on Anchored CFRP Systems. *J. Compos. Constr.* **2019**, *23*, 04019033. [[CrossRef](#)]
35. Li, W.; Liu, W.; Yang, X.; Xing, F. Experimental Study on FRP-to-Concrete Bonded Joints with FRP Sheet Anchor System. *Adv. Mater. Sci. Eng.* **2020**, *2020*, 2514313. [[CrossRef](#)]
36. Tatar, J.; Viniarski, C.; Ishfaq, M.; Harries, K.; Head, M. Effect of U-Wrap Anchors on Flexural Behavior of Reinforced Concrete Beams Flexurally Strengthened with Externally Bonded CFRP Sheets. *J. Compos. Constr.* **2023**, *27*, 04022099. [[CrossRef](#)]
37. Zhang, J.; Li, H.; Liu, S.; Sun, L.; Yang, C.; Zhang, R. Effects of Sulfate and Freeze–Thaw Cycles on the Bond Behavior of CFRP-Concrete Interface. *Constr. Build. Mater.* **2023**, *368*, 130368. [[CrossRef](#)]
38. Al-Lami, K.; Colombi, P.; D’Antino, T. Experimental and Numerical Analysis of CFRP-Concrete Joint Bond Behavior after Exposure to Wet-Dry Cycles. *Compos. Struct.* **2023**, *303*, 116273. [[CrossRef](#)]
39. Yin, Y.; Zhang, J.; Zhang, G. Effect of Hygrothermal Acid Rain Environment on the Shear Bonding Performance of CFRP-Concrete Interface. *Constr. Build. Mater.* **2023**, *364*, 130002. [[CrossRef](#)]
40. Kim, Y.; Quinn, K.; Satrom, N.; Garcia, J.; Sun, W.; Ghannoum, W.M.; Jirsa, J.O. *Shear Strengthening of Reinforced and Prestressed Concrete Beams Using Carbon Fiber Reinforced Polymer (CFRP) Sheets and Anchors*; Center for Transportation Research: Austin, TX, USA, 2012.
41. Kim, C.; Ghannoum, W.M.; Jirsa, J.O. Behavior of Reinforced Concrete Panels Strengthened with Carbon Fiber-Reinforced Polymers. *ACI Struct. J.* **2016**, *113*, 1077. [[CrossRef](#)]
42. Alotaibi, N.K. *Shear Strengthening of Reinforced Concrete Beams with Bi-Directional Carbon Fiber Reinforced Polymer (CFRP) Strips and CFRP Anchors*; The University of Texas at Austin: Austin, TX, USA, 2014.
43. Kim, C.H. *Performance of Concrete Panels Strengthened Using Carbon Fiber Reinforced Polymers (CFRP)*; The University of Texas at Austin: Austin, TX, USA, 2014.
44. Kim, C.; Jirsa, J.O.; Ghannoum, W.M. Performance of Concrete Panels Reinforced with Carbon Fiber–Reinforced Polymer Materials. *J. Compos. Constr.* **2017**, *21*, 04016100. [[CrossRef](#)]
45. Haroon, M.; Moon, J.S.; Kim, C. Performance of Reinforced Concrete Beams Strengthened with Carbon Fiber Reinforced Polymer Strips. *Materials* **2021**, *14*, 5866. [[CrossRef](#)]
46. Rasheed, H.A.; Zaki, M.A.; Foerster, A.S. Efficient Bidirectional U-Wrap System to Anchor CFRP Sheets Bonded to Reinforced Concrete T-Girders. *Structures* **2022**, *38*, 226–236. [[CrossRef](#)]
47. Kalfat, R.; Jumaah, R.; Al-Mahaidi, R.; Abdouka, K.; Hashemi, J. Post-Tensioned Concrete Beams Strengthened in Shear Using Fiber-Reinforced Polymer Laminates and Patch Anchors. *J. Compos. Constr.* **2020**, *24*, 04019065. [[CrossRef](#)]
48. Yilmaz, T.; Kiraç, N.; Anil, Ö.; Erdem, R.T.; Sezer, C. Low-Velocity Impact Behaviour of Two Way RC Slab Strengthening with CFRP Strips. *Constr. Build. Mater.* **2018**, *186*, 1046–1063. [[CrossRef](#)]
49. Al-Atta, B.; Kalfat, R.; Al-Mahaidi, R.; Al-Mosawe, A. Mitigation of IC Debonding in FRP-Plated Concrete Slabs Using Patch Anchors. *Eng. Struct.* **2020**, *214*, 110626. [[CrossRef](#)]
50. Committee, A.C.I. *Building Code Requirements for Structural Concrete and Commentary (ACI 318-19)*; American Concrete Institute: Farmington Hills, MI, USA, 2019; Volume 623.
51. Committee, A.C.I. *Building Code Requirements for Structural Concrete (ACI 318-14)*; American Concrete Institute: Farmington Hills, MI, USA, 2014.
52. Committee, A.C.I. *Guide for the Design and Construction of Externally Bonded FRP Systems for Strengthening Concrete Structures (ACI 440.2 R-17)*; American Concrete Institute: Farmington Hills, MI, USA, 2017.
53. Cervenka, V.; Cervenka, J.; Pukl, R. ATENA—A Tool for Engineering Analysis of Fracture in Concrete. *Sadhana* **2002**, *27*, 485–492. [[CrossRef](#)]
54. Alkurdi, Z. Evaluation of Pre-Tensioned Prestressed Concrete Beam Behavior by Finite Element Analysis Using ATENA 3D. In Proceedings of the 7th International Conference on Civil Structural and Transportation Engineering (ICCSTE’22), Niagara Falls, ON, Canada, 5–7 June 2022.
55. Ayub, T.; Shafiq, N.; Nuruddin, M.F.; Khan, S.U. Flexural Behaviour of High Performance Basalt Fibre Reinforced Concrete Beams: 3D Nonlinear Finite Element Analysis. In Proceedings of the 2014 IEEE Colloquium on Humanities, Science and Engineering (CHUSER 2014), Penang, Malaysia, 7–9 April 2014.

56. Le Hoang, A.; Fehling, E.; Ismail, M. Numerical Modelling of Circular Concrete Filled Steel Tube Stub Columns under Concentric Loading. In Proceedings of the 4th International Symposium on Ultra-High Performance Concrete and High Performance Construction Materials, Kassel, Germany, 9–11 March 2016.
57. Abed, M.A.; Alkurdi, Z.; Fořt, J.; Černý, R.; Solyom, S. Bond Behavior of FRP Bars in Lightweight SCC under Direct Pull-Out Conditions: Experimental and Numerical Investigation. *Materials* **2022**, *15*, 3555. [[CrossRef](#)]
58. Masne, N.; Suryawanshi, S. Analytical and Experimental Investigation of Recycled Aggregate Concrete Beams Subjected to Pure Torsion. *Int. J. Eng.* **2022**, *35*, 1959–1966. [[CrossRef](#)]
59. Kalfat, R.; Al-Mahaidi, R. Numerical and Experimental Validation of FRP Patch Anchors Used to Improve the Performance of FRP Laminates Bonded to Concrete. *J. Compos. Constr.* **2014**, *18*, A4013008. [[CrossRef](#)]

Disclaimer/Publisher's Note: The statements, opinions and data contained in all publications are solely those of the individual author(s) and contributor(s) and not of MDPI and/or the editor(s). MDPI and/or the editor(s) disclaim responsibility for any injury to people or property resulting from any ideas, methods, instructions or products referred to in the content.